Coupled chemo-mechanical behaviour of unsaturated clayey soils

X. LEI[a], H. WONG[b], A. FABBRI[c] , A. LIMAM[d] , Y. M. CHENG [e]

a. LGCB-LTDS-INSA Lyon (xiaoqin.lei@entpe.fr)
b. LGCB-LTDS-ENTPE (kwaikwan.wong@entpe.fr)
c. LGCB-LTDS-ENTPE (antonin.fabbri@entpe.fr)
d. LGCIE-INSA Lyon (ali.limam@insa-lyon.fr)
e. Polytechnic University of Hong Kong (Yung-ming.cheng@polyu.edu.hk)

Abstract :

Based on the modified mixture theory and volume fraction concept, this work presents a theoretical framework used to model coupled chemo-mechanical behaviours. The Clausius-Duhem inequality, which governs the dissipation associated with mechanical work, phase transformation, mass transport and thermal transport, is rigorously derived. According to this theoretical framework, the chemo-elastic-plastic model developed by Loret et al. (2002) for saturated homoinonic expansive clay is extended to the general unsaturated case. The model is validated against limited experimental data of oedometer tests concerning mechanical and chemo-mechanical mixed loading under controlled matric suction on reconstituted Boom Clay mixed with $NaNo_3$ solution. Reasonable and quantitative responses of these complex coupled geochemical loading paths can be obtained, and thus give us a preliminary insight on chemo-hydro-mechanical coupled behaviour.

Keywords: Thermodynamics, Multi-species mixture, Chemo-mechanical, Unsaturated expensive soil

1 Introduction

Due to their favourable characteristics such as extremely low hydraulic permeability and high swelling potential, expansive clays are widely used as sealing materials in geotechnical and geo-environment engineering, such as bentonite buffers in nuclear waste repositories and clay barriers for urban-waste landfills. However these clays are sensitive to pore water chemical compositions and matric suction changes. During their long-term service in the natural environment, these changes are inevitable. From a practical point of view, we need to understand how these changes will influence the mechanical stability and sealing ability of these barriers.

To address this complex problem, a rigorous thermodynamic framework (Lei et al., 2014) that is well adapted for formulation of coupled multi-physics phenomena for unsaturated porous media is presented in this paper. Based on this thermodynamic framework, we extend Loret et al. (2002)'s chemo-mechanical model for saturated expansive clays to account for matric suction effects. Then the model is validated against available experimental data of oedometer tests concerning mechanical and chemo-mechanical mixed loadings under controlled matric suction on reconstituted Boom Clay mixed with $NaNo_3$ solution.

2 Soil structure of unsaturated smectite

The properties of unsaturated expansive soils are strongly related to their special soil structures. A typical representative structure for these soils can be described at two structural levels as shown by Figure 1. At the macroscopic level, the soil is considered as a complex of clay aggregates, separated by inter-aggregate pores filled by either gas or free water; Water in inter-aggregate pores is free to move (free water) and is dominated by capillary forces. Inside each aggregate, the microstructural system consists of several clay particles. Each particle contains several layers. Water can reside in the inter-layers or attach to the surface of these clay particles. Being strongly bonded to the clay particles, this water will not migrate nor evaporate except when subjected to very large forces (absorbed water). Accordingly, they will be treated as parts of solid phase. However, absorbed water and free water can exchange mass with each other to reach a thermodynamic equilibrium state. And this phase change process is treated as chemical reaction in our study.

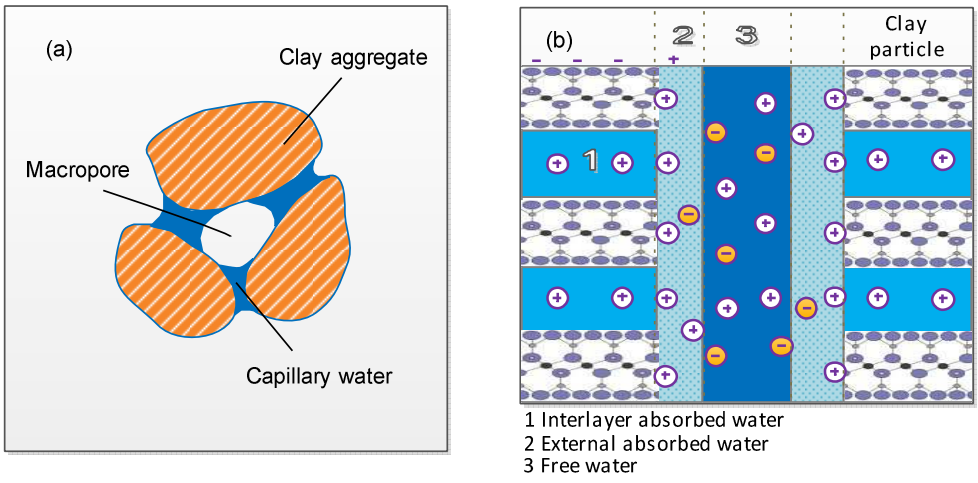

Figure 1 Macro-structure (a) and microstructure (b) of an unsaturated smectite

3 Theoretical framework

3.1 Mixture theory and volume fractions

Mathematically, the unsaturated expansive clay is treated as a three-phase multi-species porous medium. As shown in Figure 2, this tri-phasic porous medium, which occupies a volume $d\Omega_t$ in the current configuration, is taken as a representative elementary volume in this work. The solid phase $\mathcal{S}$, liquid phase $\mathcal{L}$, and gaseous phase $\mathcal{G}$ with their respective species can be summarised by the following sets:

$$\mathcal{S}=\{\mathrm{c}',\mathrm{w}',\mathrm{s}_i'\},\mathcal{L}=\{\mathrm{w},\mathrm{s}_i\},\mathcal{G}=\{\mathrm{g}\};\mathcal{A}=\mathcal{S}\cup\mathcal{L}\cup\mathcal{G};\mathcal{F}=\mathcal{L}\cup\mathcal{G} \tag{1}$$

where "c'" is the solid clay species, "w" is the water species, "s_i" is the i-th salt species, and "g" is the air species. The superscript "$'$" indicates species that are attached to the solid phase, whereas no superscript is used to refer to species within the fluid phases. For example, "w" refers to the free water in the liquid phase, and "w'" refers to the absorbed water attached to the solid phase, whereas "$\mathcal{A}$" is used to denote the entire set of all species within the porous medium, and "$\mathcal{F}$" is used to denote the set of species that compose the fluid phases.

To describe the preferential exchange of species between solid phase $\mathcal{S}$ and liquid phase $\mathcal{L}$ that arises from the physical-chemical reactions, a fictitious semi-permeable membrane is assumed to surround the cluster of clay platelets, which is a priori impermeable to clay species c'. However, here the exchange between liquid water and water vapour is neglected by assuming that dry air is the only species in the gaseous phase. To facilitate the frequent reference of the exchangeable species, the following sets of exchangeable species are defined:

$$\mathcal{S}^{\leftrightarrow}=\{\mathrm{w}',\mathrm{s}_i'\},\mathcal{C}=\{\mathrm{w},\mathrm{s}_i\} \tag{2}$$

Based on mixture theory, this three-phase porous medium can be treated as the superposition of three continua, one solid and two fluids. These continua are assumed to simultaneously occupy the entire physical domain but with reduced densities to maintain the overall mass balance. Take the solid continua for example. The solid matrix has the intrinsic density ρ_S with its own volume now has the apparent density ρ^S over the whole porous volume. The volume fractions (such as porosity n) and saturations (such as the liquid saturation $S_{\mathcal{L}}$ and the gas saturation S_g) are introduced to interchange these two densities, as shown in Figure 2. By the same procedure, the multi-species porous medium can also be treated as the superposition of multiple species continua.

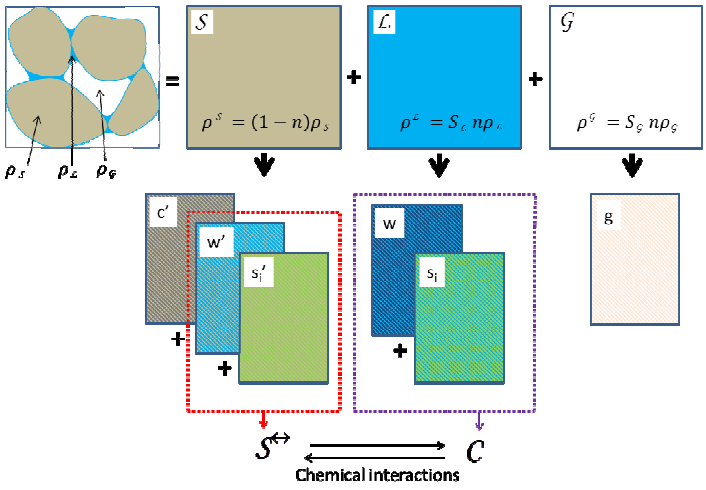

Figure 2 Representation of an unsaturated porous medium as a superimposed mixture: (top) three-phase macroscopic model of the REV; (bottom) multiple-species macroscopic model of the REV

3.2 Irreversible thermodynamics

Irreversible thermodynamics can provide an efficient description of the coupled processes. In the framework of classical continuum mechanics, the balance laws governing mass, momentum, energy and entropy can be derived. Based on energy and entropy balance laws, the Clausius-Duhem inequality associated with the above open thermodynamic tri-phasic clay system consisting of a solid-liquid-gas mixture has been derived in Lei et al. (2014), and is presented by Equation (3). This Clausius-Duhem inequality states that the dissipation Φ of a thermodynamically viable process must be non-negative. For our multi-physical problems, we assume that this dissipation can be decomposed into dissipations associated with mechanical work Φ_m, phase change Φ_{pc}, mass transport Φ_{tr}, and thermal transport Φ_{th}. Each contribution will be required to be positive in our study.

$$\Phi = \Phi_m + \Phi_{pc} + \Phi_{tr} + \Phi_{th} \geq 0 \tag{3}$$

With

$$\Phi_m = \boldsymbol{\sigma} : \frac{d^s}{dt}\boldsymbol{\varepsilon} + \sum_{k\in\mathcal{F}} \mu_k \frac{d^s}{dt} m_k + \sum_{k'\in\mathcal{S}^{\leftrightarrow}} \mu_{k'} \frac{d^s}{dt} m_{k'} - \eta \frac{d^s}{dt} T - \frac{d^s}{dt}\Psi \geq 0 \tag{4}$$

$$\Phi_{pc} = -\sum_{\substack{k\in\mathcal{C} \\ k'\in\mathcal{S}^{\leftrightarrow}}} \left(\mu_k - \mu_{k'}\right)\hat{m}_k \geq 0 \tag{5}$$

$$\Phi_{tr} = -\sum_{k\in\mathcal{F}} \boldsymbol{I}^k \cdot \left[\nabla\mu_k + \eta_k \nabla T\right] \geq 0 \tag{6}$$

$$\Phi_{th} = -\frac{q\cdot\nabla T}{T} \geq 0 \tag{7}$$

Where, $\boldsymbol{\sigma}$ and $\boldsymbol{\varepsilon}$ are the Cauchy stress tensor and the linearized strain tensor, respectively; m_j and $\hat{m}_j$ are the mass content and the mass growth rate of species j per unit initial volume $d\Omega_0$; μ_j is the chemical potential per unit of mass of species j; η is the total entropy per unit of overall volume of porous medium, T is the absolute temperature, q is the heat flux vector, and Ψ is the total Lagrangian free energy.

4 Constitutive law for skeleton deformation

The dissipation Φ_m presented in Equation (3) is the mechanical dissipation associated with the fluid phases and the solid skeleton, from which, the constitutive models for solid deformation can be derived. As an illustration of the applicability of the above thermodynamic framework, the chemo-elastic-plastic model developed by Loret et al. (2002) for saturated homoinonic expansive clay is extended to the general unsaturated case based on this framework.

4.1 Energy distribution

To proceed, the soil is conceptually divided into two distinct parts: the solid skeleton and the saturating fluids. The solid skeleton serves as the reference frame for the chosen representative elementary volume and is described by Lagrangian coordinates. However, the fluids can enter or leave the chosen elementary volume or even the physical domain and thus can only be described by using Eulerian coordinates.

To arrive at the formulation of the solid skeleton, we decompose the total free energy Ψ and the total entropy η in Equation (4) into two parts, one associated with the apparent solid skeleton and the other with the bulk fluids. By subtraction, the corresponding parts (Ψ_S and η_S) concerning the apparent solid skeleton can be obtained.

$$\Psi_S = \Psi - \sum_{\alpha=L,G} \Psi_\alpha ; \eta_S = \eta - \sum_{\alpha=L,G} \eta_\alpha \tag{8}$$

From the energy point of view, the apparent solid skeleton can be further viewed as comprising the solid skeleton and the interfaces. And each part has its own associated free energy (Coussy, 2004). During a general process in which irreversible energy transfer may occur, the work input to this system is partially stored as free energy in the solid skeleton and the solid-fluids interfaces and partially dissipated (Coussy, 2004). To proceed, the solid skeleton is assumed to be decoupled from its attached interfaces by assuming the solid skeleton (sol) and the interfaces (int) have their own associated dissipations and free energies:

$$\Phi_m = \Phi_{sol} + \Phi_{\text{int}} ; \Psi = \Psi_{sol} + \Psi_{\text{int}} \tag{9}$$

In addition, free energy Ψ may include the elastic free energy (reversible, indicated by superscript "e") Ψ^e and locked energy Ψ^p (stored during previous irreversible process, for its release must be accompanied by dissipative process, indicated by superscript "p"). And this is the case for both the free energy of solid skeleton and that of interfaces. Consequently, the free energy can be further decomposed into:

$$\Psi = \Psi_{sol} + \Psi_{\text{int}} = \Psi^e_{sol} + \Psi^p_{sol} + \Psi^e_{\text{int}} + \Psi^p_{\text{int}} \tag{10}$$

In this work, the following dependency of the free energy is assumed (Lei et al., 2015).

$$\Psi = \Psi^e_{sol}\left(\boldsymbol{\varepsilon}^e, m^e_{w'}, S_L\right) + \Psi^p_{sol}\left(\xi_{sol}, S_L\right) + \Psi^e_{\text{int}}\left(S^e_L, \boldsymbol{\varepsilon}\right) + \Psi^p_{\text{int}}\left(\xi_{\text{int}}, \boldsymbol{\varepsilon}\right) \tag{11}$$

Where ξ_{sol} and ξ_{int} are two internal variables introduced to account for the hardening effects for the solid skeleton and the interfaces respectively. By invoking the definitions of the generalized effective stresses $\bar{\boldsymbol{\sigma}}$ and the effective chemical potential of absorbed water $\bar{\mu}_{w'}$ (Lei et al., 2014):

$$\bar{\boldsymbol{\sigma}} = \boldsymbol{\sigma} + p^* \boldsymbol{1}; \ \bar{\mu}_{w'} = \mu_{w'} - \frac{p^*}{\rho_{w'}} \tag{12}$$

With the equivalent pore pressure p^* defined by $p^* = \chi p_L + (1-\chi) p_G$, in which χ serves as the Bishop's parameter. Accordingly, the Clausius-Duhem inequality (4) can be rewritten in the following form (Lei et al., 2015):

$$\begin{aligned} \Phi_m = & \left[\left(\bar{\boldsymbol{\sigma}} : d\boldsymbol{\varepsilon}^e + \bar{\mu}_{w'} dm^e_{w'} - d\Psi^e_{sol}\right) + \left(-\beta_{sol} d\xi_{sol} - d\Psi^p_{sol}\right)\right] \\ & + \left[\left(-\phi_0 s dS^e_L - d\Psi^e_{\text{int}}\right) + \left(-\beta_{\text{int}} d\xi_{\text{int}} - d\Psi^p_{\text{int}}\right)\right] \\ & + \left(\bar{\boldsymbol{\sigma}} : d\boldsymbol{\varepsilon}^p + \bar{\mu}_{w'} dm^p_{w'} + \beta_{sol} d\xi_{sol}\right) + \left(-\phi_0 s dS^p_L + \beta_{\text{int}} d\xi_{\text{int}}\right) \geq 0 \end{aligned} \tag{13}$$

Where, ϕ_0 is the initial porosity, s is the matric suction, β_{sol} and β_{int} are the hardening forces which are energetically conjugated to their corresponding hardening variables, and are defined by

$$\beta_{sol} = -\left(\frac{\partial \Psi^{p}_{sol}}{\partial \xi_{sol}}\right)_{S_{\mathcal{L}}} ; \beta_{\text{int}} = -\left(\frac{\partial \Psi^{p}_{\text{int}}}{\partial \xi_{\text{int}}}\right)_{\boldsymbol{\varepsilon}} \tag{14}$$

The terms in the first parentheses in the two brackets of equation (13) imply that the elastic work input are stored as elastic free energies for the solid skeleton and interfaces respectively. They can be rewritten as:

$$d\Psi^{e}_{sol} = \overline{\boldsymbol{\sigma}} : d\boldsymbol{\varepsilon}^{e} + \overline{\mu}_{w'} dm^{e}_{w'} \tag{15}$$

$$d\Psi^{e}_{\text{int}} = -\phi_0 s dS^{e}_{\mathcal{L}} \tag{16}$$

Considering the state equation (14), the following two Clausius-Duhem inequalities should be satisfied at the same time:

$$\Phi_{sol} = \overline{\boldsymbol{\sigma}} : d\boldsymbol{\varepsilon}^{p} + \overline{\mu}_{w'} dm^{p}_{w'} + \beta_{sol} d\xi_{sol} \geq 0 \tag{17}$$

$$\Phi_{\text{int}} = -\phi_0 s dS^{p}_{\mathcal{L}} + \beta_{\text{int}} d\xi_{\text{int}} \geq 0 \tag{18}$$

The elastic free energy equations (15) and (17) are the starting point to build reversible state laws and the dissipation equations (16) and (18) will provide governing laws for plastic behaviours. In what follows, only the constitutive model for solid skeleton deformation will be presented.

4.2 Chemo-hyperelastic model

In tri-axial stress state, the strain work expression in equation (15) can be altered accordingly:

$$d\Psi^{e}_{sol} = \overline{p} d\varepsilon^{e}_{v} + q d\varepsilon^{e}_{s} + \overline{\mu}_{w'} dm^{e}_{w'} \tag{19}$$

In which, the effective stresses $\overline{\boldsymbol{\sigma}}$ and strain $\boldsymbol{\varepsilon}$ are replaced with the volumetric strain ε^{e}_{v}, equivalent strain ε^{e}_{s}, effective stress $\overline{p}$, Mises equivalent stress q. For the construction of the elastic-plastic model, it is more convenient to treat the stresses as independent variables rather than the strains. To this end, the differential of free energy Ψ^{e}_{sol} can be transformed using a partial Legendre transform as:

$$d\overline{\Psi}^{e}_{sol}\left(\overline{p}, q, m^{e}_{w'}\right) = d\left(\overline{p}\varepsilon^{e}_{v} + q\varepsilon^{e}_{s} - \Psi^{e}_{sol}\right) = \varepsilon^{e}_{v} d\overline{p} + \varepsilon^{e}_{s} dq - \overline{\mu}_{w'} dm^{e}_{w'} \tag{20}$$

which relates the generalised stress variables $\left(\overline{p}, q, \overline{\mu}_{w'}\right)$ to their work-conjugate counterparts, the generalised strain variables $\left(\varepsilon^{e}_{v}, \varepsilon^{e}_{s}, m^{e}_{w'}\right)$.

Now let $\overline{p}_0$ denote a small reference value with the pore fluid as distilled water under purely mechanical loading during the elastic deformation, and the slope of an over consolidation line (OCL) is κ^{w}. After chemical loading, the slope of this OCL becomes κ, and it intersects the original OCL at the point corresponding to the effective stress $\overline{p}_{\kappa}$. Following Loret et al. (2002), the expression of the skeleton free energy Ψ^{SK} is assumed as (Lei et al., 2014):

$$\Psi^{SK} = \overline{p}\kappa^{w} \ln\frac{\overline{p}_{\kappa}}{\overline{p}_0} + \kappa\overline{p}\left(\ln\frac{\overline{p}}{\overline{p}_{\kappa}} - 1\right) + \frac{q^2}{6G} - \mu^{0}_{w'} m^{e}_{w'} - \frac{RT}{V_0}\left(N_{w'} \ln N_{w'} - N_S \ln N_S\right) \tag{21}$$

In the above, R is the universal gas constant, $\mu_{w'}^0$ is the reference chemical potential, $\mathcal{M}_{w'}$ is the molar mass of absorbed water, and $x_{w'} = {N_{w'}}/{N_S}$ is the molar fraction of the absorbed water species with $N_{w'}$ and N_S denoting the molar quantities of absorbed water species and all solid phase species, respectively, within the original volume V_0. Now, an incremental chemo-poro-elastic constitutive model can be expressed as:

$$\begin{bmatrix} d\varepsilon_v^e \\ d\varepsilon_s^e \\ d\bar{\mu}_{w'} \end{bmatrix} = \begin{bmatrix} \frac{\partial^2 \Psi^{SK}}{\partial \bar{p}^2} & \frac{\partial^2 \Psi^{SK}}{\partial \bar{p} \partial q} & \frac{\partial^2 \Psi^{SK}}{\partial \bar{p} \partial m_{w'}^e} \\ \frac{\partial^2 \Psi^{SK}}{\partial q \partial \bar{p}} & \frac{\partial^2 \Psi^{SK}}{\partial q^2} & \frac{\partial^2 \Psi^{SK}}{\partial q \partial m_{w'}^e} \\ \frac{\partial^2 \Psi^{SK}}{\partial m_{w'}^e \partial \bar{p}} & \frac{\partial^2 \Psi^{SK}}{\partial m_{w'}^e \partial q} & \frac{\partial^2 \Psi^{SK}}{\partial m_{w'}^{e\,2}} \end{bmatrix} \begin{bmatrix} d\bar{p} \\ dq \\ dm_{w'}^e \end{bmatrix} \tag{22}$$

Based on the fact that elastic coefficient κ is dependent on the mass contents of the absorbed water $m_{w'}^e$, and by assuming that Poisson's ratio is independent of $m_{w'}^e$, after selected arrangement, another form taking $\boldsymbol{\Sigma} = \left[\bar{p}, q, -\bar{\mu}_{w'}\right]^T$ as generalised stress-like variables and $\boldsymbol{E}^e = \left[\varepsilon_v^e, \varepsilon_s^e, m_{w'}^e\right]^T$ as generalised elastic strain-like variables can be obtained as

$$\dot{\boldsymbol{\Sigma}} = \boldsymbol{D}^e \dot{\boldsymbol{E}}^e \tag{23}$$

With

$$\boldsymbol{D}^e = \begin{bmatrix} D_{uu} & 0 & D_{um} \\ 0 & 3G & 0 \\ D_{mu} & 0 & D_{mm} \end{bmatrix}$$

In which,

$$D_{uu} = \frac{\bar{p}}{\kappa}; D_{um} = -\frac{\bar{p}}{\kappa} \ln \frac{\bar{p}}{\bar{p}_\kappa} \frac{d\kappa}{dm_{w'}^e} = D_{mu}; D_{mm} = \frac{\bar{p}}{\kappa} \left(\ln \frac{\bar{p}}{\bar{p}_\kappa} \frac{d\kappa}{dm_{w'}^e} \right)^2 + \bar{p} \left(1 - \ln \frac{\bar{p}}{\bar{p}_\kappa} \right) \frac{d^2\kappa}{dm_{w'}^{e\,2}} + \frac{RT}{\mathcal{M}_{w'}} \frac{1}{x_{w'}} \frac{dx_{w'}}{dm_{w'}^e}$$

4.3 Elasto-plastic model

Using the Cam-Clay notation, the solid skeleton dissipation (17) can be rewritten as:

$$\Phi_{sol} = \bar{p} d\varepsilon_v^p + q d\varepsilon_s^p + \bar{\mu}_{w'} dm_{w'}^p + \beta_{sol} d\xi_{sol} \geq 0 \tag{24}$$

Based on the above equation, the principle of maximum plastic dissipation implies the following normality flow rule

$$d\varepsilon_v^p = d\lambda \frac{\partial g}{\partial \bar{p}}; d\varepsilon_s^p = d\lambda \frac{\partial g}{\partial q}; dm_{w'}^p = d\lambda \frac{\partial g}{\partial \bar{\mu}_{w'}} \tag{25}$$

where $d\lambda \geq 0$ is the plastic multiplier, and g is the plastic potential. For simplicity, the plastic potential g is set equal to the yield function f introduced below. Thus an associated flow rule is assumed, and the thermodynamic consistency is automatically satisfied (Coussy, 2004). In addition, equation (24) also leads to the normality flow rule for the hardening variable

$$d\xi_{sol} = d\lambda \frac{\partial g}{\partial \beta_{sol}} \tag{26}$$

Consistent with the classic plasticity theory, it is assumed that a yield surface exists for the unsaturated expansive soil representing the boundary of the elastic region:

$$f = f\left(\bar{p}, q, \bar{\mu}_{w'}, \beta_{sol}\right) = 0 \tag{27}$$

where the choice of the independent arguments are motivated by the dissipation inequality (24) comprising state variables $\bar{p}, q, \bar{\mu}_{w'}$ and the hardening parameter β_{sol}. A general form taking $\boldsymbol{\Sigma} = \left[\bar{p}, q, -\bar{\mu}_{w'}\right]^T$ as generalised stress-like variables and $\boldsymbol{E} = \left[\varepsilon_v, \varepsilon_s, m_{w'}\right]^T$ as generalised strain-like variables can be written as

$$\dot{\boldsymbol{\Sigma}} = \left(\boldsymbol{D}^e - \boldsymbol{D}^p\right)\dot{\boldsymbol{E}} \tag{28}$$

During plastic loading, the stress point is always on the yield surface ($f = 0$) and the consistency condition ($df = 0$) should be satisfied at the same time. Following the classic procedure (Coussy, 2004), the plastic stiffness $\boldsymbol{D}^p$ in the above equation can be solved as

$$\boldsymbol{D}^p = \frac{\boldsymbol{D}^e \left[\frac{\partial g}{\partial \boldsymbol{\Sigma}}\right]^t \left[\frac{\partial f}{\partial \boldsymbol{\Sigma}}\right] \boldsymbol{D}^e}{A + {}^t\left[\frac{\partial g}{\partial \boldsymbol{\Sigma}}\right] \boldsymbol{D}^e \left[\frac{\partial f}{\partial \boldsymbol{\Sigma}}\right]} \tag{29}$$

where A is the hardening modulus, and is obtained by (Coussy, 2004)

$$A = -\frac{\partial f}{\partial \beta_{sol}} \frac{\partial \beta_{sol}}{\partial \xi_{sol}} \frac{\partial \xi_{sol}}{\partial \lambda} = \frac{\partial f}{\partial \beta_{sol}} \frac{\partial^2 \Psi^p_{sol}}{\partial {\xi_{sol}}^2} \frac{\partial g}{\partial \beta_{sol}} \tag{30}$$

The modified Cam-Clay model is adopted as the base model, with the yield surface:

$$f = \frac{q^2}{M^2 \bar{p}} + \bar{p} - \bar{p}_c = 0 \tag{31}$$

where M is the slope of the critical state line, and $\bar{p}_c$ is the preconsolidation stress which classically depends on the volumetric plastic strain ε_v^p. To account for the influence of suction and pore water chemical concentration, M is assumed to be dependent on pore water salt concentration as addressed by Loret et al. (2002). Concerning $\bar{p}_c$, besides the dependency on volumetric plastic strain ε_v^p, it is also strongly dependent on matric suction s and pore water salt concentration c_s:

$$\bar{p}_c = \bar{p}_{co} \exp\left(\frac{\varepsilon_v^p}{\lambda - \kappa}\right) h(s, x_{w'}) \tag{32}$$

With

$$h(s, x_{w'}) = \left(\frac{\overline{p}_\lambda}{\overline{p}_{co}} \right)^{\left(1-\frac{\lambda^w-\kappa^w}{\lambda-\kappa}\right)} \left(\frac{\overline{p}_\lambda}{\overline{p}_k} \right)^{\left(\frac{\kappa-\kappa^w}{\lambda-\kappa}\right)} \tag{33}$$

In the above hardening law, $\overline{p}_{co}$, $\overline{p}_k$, $\overline{p}_\lambda$, κ^w and λ^w are material constants, whereas κ and λ evolve with suction s and pore water salinity c_s, and control the evolution of the preconsolidation pressure.

4 Validation

As partial validations, here we simulate a series of oedometer tests on natural Boom Clay performed by Mokni (2011). To investigate the influences of pore water salinity on mechanical properties of unsaturated Boom Clay, oedometer tests on samples mixed with 0 M, 4 M, 5.4 M $NaNo_3$ under 500 kPa matric suction have also been performed. As can be seen in Figure 3, when mechanically loaded under various $NaNo_3$ concentrations, the properties of samples under 500 kPa matric suction varied following the same tendencies as the ones in saturated state (see experimental data presented in Loret et al. (2002) and Mokni (2011)): compression index increases with chemical concentration; swelling index shows a negligible increase; at low salinity level, chemical softening dominates; at larger salinity levels, chemical induced plasticity is triggered and strain hardening gradually dominates.

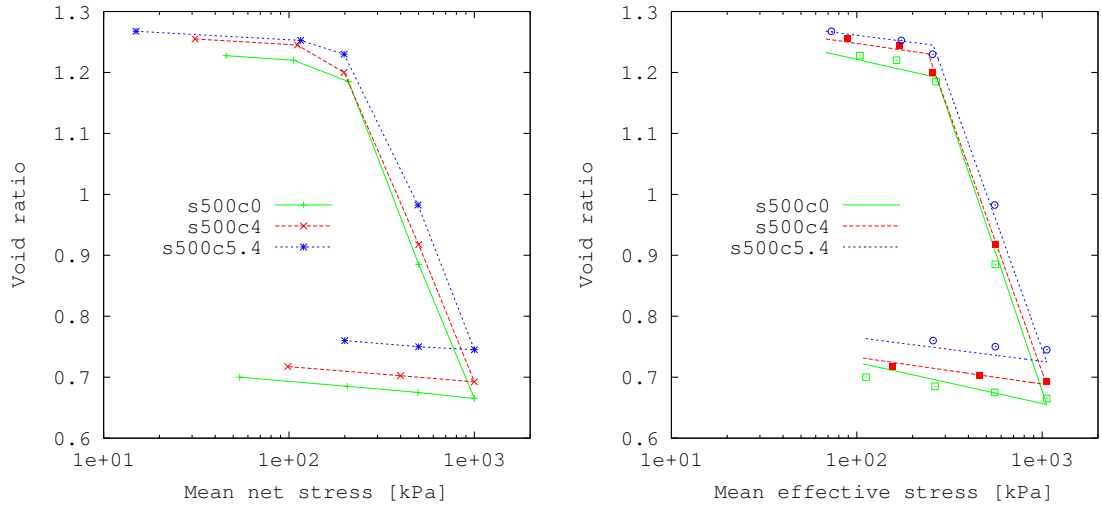

(a) Experimental results (Mokni, 2011); (b) Numerical results

Figure 3 Oedometer tests on Boom Clay samples mixed with 0M, 4M, 5.4M NaNo3 under constant suction 500 kPa

In addition, mixed chemo-mechanical loading paths have also applied on unsaturated Boom Clay samples with 500 kPa suction, as can be seen in Figure 4. Similar to the samples tested under null suction (see experimental data presented in Loret et al. (2002) and Mokni (2011)), when subjected to 6.53M chemical loading at 100 kPa, a significant volume contraction (about 3.8%) was observed on the Boom Clay with 500 kPa suction, and a decrease of compressibility was also observed on subsequent loading. After a mechanical loading up to 1000 kPa, the sample was unloaded again to 100 kPa. Similarly to the saturated case, an insignificant swelling was observed when the sample is exposed to distilled water at this stress level.

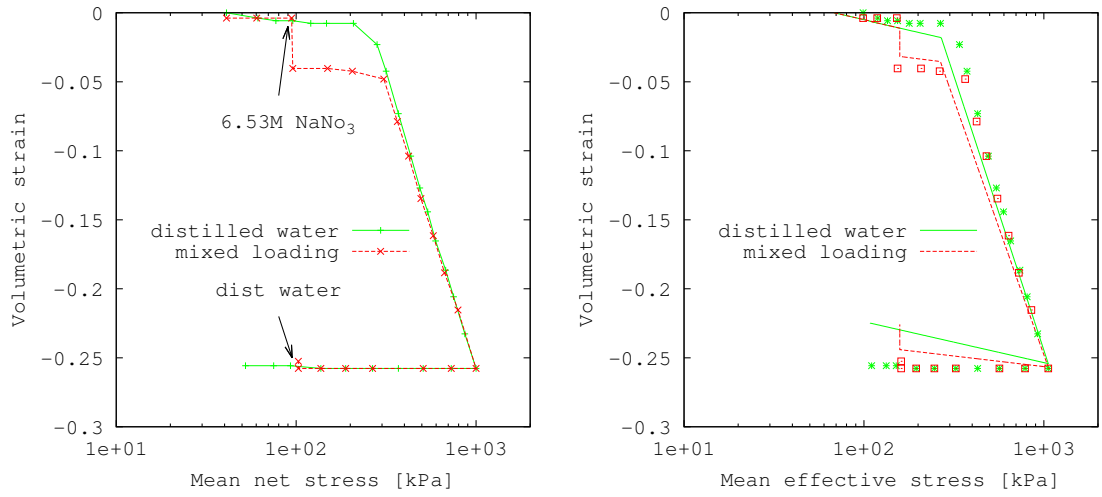

(a) Experimental results (Mokni, 2011); (b) Numerical results

Figure 4 Mixed mechanical-chemical loading cycle on unsaturated samples with suction 500 kPa: 6.53 M chemical loading at 100 kPa vertical stress, after mechanical loading-unloading, then exposed to distilled water at vertical stress 100 kPa

These tendencies of unsaturated Boom Clay under mechanical and mixed chemo-mechanical loadings presented above are similar to those of saturated Boom Clay and are relatively well captured by the model predictions, thus can partially support our extension of the chemo-mechanical saturated model to the unsaturated model by following those classic approaches used for chemically insensitive soils.

5 Conclusion

Based on the modified mixture theory and the theory of non-equilibrium thermodynamics, a theoretical framework was developed to model the chemo-poro-mechanical coupled behaviour of partially saturated expansive clays. Then according to this thermodynamic framework, Loret et al. (2002)'s chemo-mechanical elastic-plastic model for saturated expansive clays was extended to the general unsaturated case. The extended model accounts for chemical and suction effects by relating the mechanical properties to the evolution of molar fraction of absorbed water and matric suction. The joint effects of pore water chemistry and matric suction on preconsolidation stress are automatically taken into consideration according to the evolution of the resulting mechanical properties. The model is then used to reproduce oedometer tests on unsaturated Boom Clay involving both mechanical and chemo-mechanical mixed loading paths. Compared to the experimental results, in spite of the complexity of the coupled multi-mechanisms involved, the predictions obtained by the model proposed is quite satisfying.

References

[1] Coussy, O., 2004. Poromechanics. John Wiley & Sons, Ltd.

[2] Lei, X., Wong, H., Fabbri, A., Limam, A., Cheng, Y.M., 2014. A thermo-chemo-electro-mechanical framework of unsaturated expansive clays. Comput. Geotech. 62, 175–192.

[3] Lei, X., Wong, H., Fabbri, A., Limam, A., Cheng, Y.M., 2015. A chemo-elastic-plastic model for unsaturated expansive clay. Submitted for publication.

[4] Loret, B., Hueckel, T., Gajo, A., 2002. Chemo-mechanical coupling in saturated porous media: elastic–plastic behaviour of homoionic expansive clays. Int. J. Solids Struct. 39, 2773–2806.

[5] Mokni, N., 2011. Deformation and flow driven by osmotic processes in porous materials. PhD thesis. Technical University of Catalunya, UPC.